



## Discovery of benzimidazole pyrrolidinyl amides as prolylcarboxypeptidase inhibitors

Hong C. Shen<sup>a,\*</sup>, Fa-Xiang Ding<sup>a</sup>, Changyou Zhou<sup>a</sup>, Yusheng Xiong<sup>a</sup>, Andreas Verras<sup>a</sup>, Renee M. Chabin<sup>b</sup>, Suoyu Xu<sup>c</sup>, Xinchun Tong<sup>c</sup>, Dan Xie<sup>d</sup>, Michael E. Lassman<sup>d</sup>, Urmi R. Bhatt<sup>d</sup>, Margarita M. Garcia-Calvo<sup>d</sup>, Wayne Geissler<sup>d</sup>, Zhu Shen<sup>d</sup>, Dunlu Chen<sup>d</sup>, Ranabir SinhaRoy<sup>d</sup>, Jeffery J. Hale<sup>a</sup>, James R. Tata<sup>a</sup>, Shirley Pinto<sup>d</sup>, Dong-Ming Shen<sup>a</sup>, Steven L. Colletti<sup>a</sup>

<sup>a</sup> Department of Medicinal Chemistry, Merck Research Laboratories, PO Box 2000, Rahway, NJ 07065-0900, USA

<sup>b</sup> Department of Research Operations, Merck Research Laboratories, PO Box 2000, Rahway, NJ 07065-0900, USA

<sup>c</sup> Department of Drug Metabolism, Merck Research Laboratories, PO Box 2000, Rahway, NJ 07065-0900, USA

<sup>d</sup> Department of Metabolic Disorders, Merck Research Laboratories, PO Box 2000, Rahway, NJ 07065-0900, USA

### ARTICLE INFO

#### Article history:

Received 8 January 2011

Revised 19 January 2011

Accepted 20 January 2011

Available online 26 January 2011

#### Keywords:

PrCP

Prolylcarboxypeptidase

Inhibitors

Obesity

Benzimidazole pyrrolidinyl amides

### ABSTRACT

A series of benzimidazole pyrrolidinyl amides containing a piperidinyl group were discovered as novel prolylcarboxypeptidase (PrCP) inhibitors. Low-nanomolar IC<sub>50</sub>'s were achieved for several analogs, of which compound **9b** displayed modest ex vivo target engagement in eDIO mouse plasma. Compound **9b** was also studied in vivo for its effect on weight loss and food intake in an eDIO mouse model and the results will be discussed.

© 2011 Elsevier Ltd. All rights reserved.

Isolated from kidney extract,<sup>1</sup> and later cloned from a human kidney library,<sup>2</sup> prolylcarboxypeptidase (PrCP) belongs to a class of serine peptidases that cleaves the C-terminal amino acids linked to proline in peptides such as angiotensin II (AngII), angiotensin III (AngIII) and des-Arg9-bradykinin.<sup>3</sup> PrCP is widely expressed in various organs including kidney, lung, adipose, liver, brain, heart, pancreas, etc.<sup>4</sup> Within these organs, this enzyme is active in both lysosomes and the membrane of human alveolar macrophages.<sup>5</sup> The roles of PrCP to convert AngII to Ang 1-7 and AngIII to Ang 2-7 indicate a potential function of PrCP in both blood pressure regulation and electrolyte balance.<sup>3</sup> In addition, the human gene for PrCP (11q14) may be related to essential hypertension.<sup>6</sup>

In the past several years, significant progress has been made in understanding the potential therapeutic utility of PrCP inhibition. In 2005, the Horvath group at Yale University suggested that PrCP inhibition could lead to treatment of obesity, diabetes and related conditions.<sup>7</sup> This work is primarily based upon the PrCP  $-/-$  mouse phenotype as well as rat pharmacology with a serine trap PrCP inhibitor. It has also been reported that chromosomal region

D7Mit353, containing the PrCP gene, confers lean phenotype in mice (50% less fat).<sup>8</sup> In human genetic studies, a single cohort of PrCP single nucleotide polymorphism (SNP) was found to be associated with metabolic syndrome.<sup>9</sup> Most recently, GlaxoSmithKline also suggested the utility of PrCP inhibitors in treating obesity, based on a human SNP analysis of PrCP in 937 obese individuals. This study demonstrated a significant correlation between *PrCP* gene permutation and high body mass index (BMI) values (>30).<sup>10</sup>

To explore the potential of PrCP inhibitors in treatment of obesity,<sup>11</sup> we began to investigate whether the inhibition of PrCP indeed led to mechanism-based weight loss in obesity models. Furthermore, we attempted to understand the relevance of central and/or peripheral PrCP inhibition to any observed efficacy. Herein, we report our efforts in identifying a class of potent peripheral PrCP inhibitors, and their pharmacodynamic (PD) effects in established diet-induced obese (eDIO) wild type mice and eDIO/PrCP knockout mice.

Inspired by a potent PrCP inhibitor reported by Merck colleagues earlier (**1** in Fig. 1),<sup>12</sup> we attempted to remove both the  $\alpha$ -aminoisobutyl amide group and the  $\beta$ -methyl group in order to eliminate chiral centers and simplify the structures. Furthermore, the introduction of a cyclic secondary amine could replace the inner phenyl group of the biphenyl moiety of analog **1**, thereby

\* Corresponding author. Tel.: +1 732 594 1755; fax: +1 732 594 9473.

E-mail address: [hong\\_shen@merck.com](mailto:hong_shen@merck.com) (H.C. Shen).

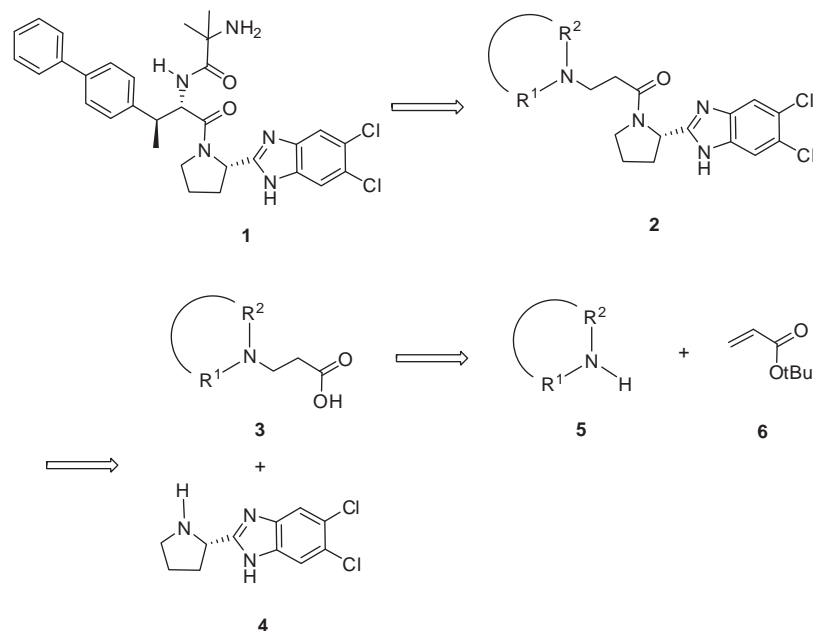


Figure 1. Design and synthesis of PrCP inhibitors.

increasing the polarity and potentially reducing the serum shift of these compounds. This simplified design of analogs also allowed for parallel synthesis and thus rapid establishment of structure–activity relationship (SAR). As shown in Figure 1, the synthesis of the analogs described as general structure 2 involved the amide coupling of  $\beta$ -amino acid 3 and benzimidazole pyrrolidine 4. The requisite  $\beta$ -amino acid 3 could then be derived from the 1,4-addition of amine 5 to *t*-butyl acrylate 6.

Besides the human PrCP inhibition assay, a subset of compounds were also tested in the mouse PrCP inhibition assay and/or the AngIII assay which was conducted in the whole mouse plasma. The AngIII assay enabled the assessment of plasma serum shift of compounds. In this assay, the mouse plasma was first treated with protease inhibitors to suppress the cleavage of AngIII by non-PrCP proteases. A PrCP inhibitor was then added to study the cleavage of AngIII in comparison with the vehicle, in which this conversion was primarily promoted by PrCP.

Aided by the human PrCP enzyme inhibition assay, the optimal ring size of the cyclic secondary amine was investigated first (Table 1, 7a–7d). 4-Phenyl piperidiny analog 7a and 4-phenyl homopiperidiny analog 7b had similar  $IC_{50}$ 's for PrCP, but compound 7a is structurally simpler by having one less chiral center compared with 7b. Compound 7a was also more potent than lower homologs 7c and 7d. In addition, piperazine analog 7e provided similar activity. However, despite the good enzyme inhibition, these compounds appeared to have an unexpectedly large serum shift, which was reflected by the mouse AngIII assay data. It was then envisioned that further replacement of the terminal phenyl group with polar heteroaryls may reduce the observed serum shifts. Thus, several analogs containing five- or six-membered heteroaryls (7f–r) were prepared. Indeed, polar pyrazolepiperidine analog 7f, and 4-pyridylpiperidine 7o led to enhanced activity in mouse whole serum ( $IC_{50}$  = 290 nM and 430 nM, respectively).

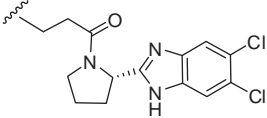
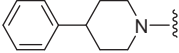
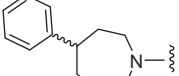
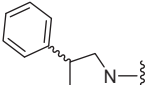
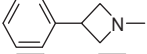
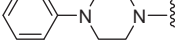
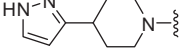
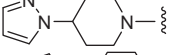
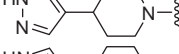
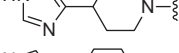
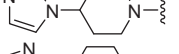
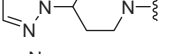
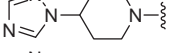
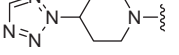
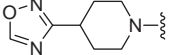
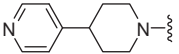
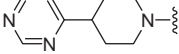
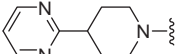
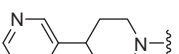
Due to the reduced serum shift, reasonable PrCP inhibitory activity of pyrazole 7f and oxadiazole 7n, their derivatives were further explored using readily available building blocks. The SAR regarding the attached aryl or heteroaryl to either of these two heteroaryls is summarized in Tables 2 and 3. Several compounds (8a, 8c, 8f, 8g, 9a, 9b, 9f) in both the oxadiazole (Table 2) and

the pyrazole (Table 3) series exhibited excellent PrCP inhibitory activity in the absence of mouse serum. In addition, polar terminal groups such as pyridyl (8c, 9b, 9c) or phenyl sulfone (8g) analogs demonstrated excellent PrCP inhibitory activity in mouse plasma ( $IC_{50}$  <40 nM). Unfortunately, modification of piperidine by adding a carbonyl group (8i) or introducing a geminal-dimethyl group (8j) did not offer significant advantages regarding PrCP inhibition, serum shift reduction, or PK profiles (Table 4) with respect to analog 8a.

Mouse pharmacokinetic (PK) profiles of compounds 8a–9b (Table 4) were characterized by high clearance, low oral bioavailability and low oral exposure. To ascertain whether compound 9b was a p-gp (p-glycoprotein) substrate, a PK study in CF1 wild type and p-gp deficient mice was conducted. At a 0.5 mpk (mg/kg) dose in CF1 wild type mice, the brain/plasma ratio was 0.20 (10 nM/54 nM) at half an hour post dosing, and 0.88 (4.0 nM/4.6 nM) at 4 h post dosing. In contrast, in mdr (multidrug resistance) 1a–/– mice with deficient p-gp transporter, the brain/plasma compound ratio was 1.4 (70 nM/51 nM) at half an hour post dosing, and 13 (54 nM/4 nM) at 4 h post dosing. Since 9b was a p-gp substrate *in vivo*, it was utilized as a tool compound to evaluate whether peripheral PrCP inhibition could lead to weight loss in eDIO mice.

To measure the *ex vivo* target engagement of 9b in plasma, the wild type eDIO mice were dosed with 9b subcutaneously (sc) using continuous infusion pumps in three different groups at 10, 30, and 60 mg/kg (mpk), respectively, for seven days. On the seventh day, compound 9b exhibited a similar target engagement in plasma at all three different doses (B, C, D in Fig. 2). Furthermore, at the 60 mpk dose, the maximum efficacy was not achieved. The highest inhibition observed was 55% for group D versus 80% for group D+, in which 2  $\mu$ M of added compound 9b provided additional PrCP inhibition. The similar plasma levels of 9b in all three groups (0.09–0.16  $\mu$ M) explained why there was a lack of optimal target engagement despite higher doses. The lack of improvement of drug exposure in spite of increasing dosage was most likely due to the observed compound precipitation during the subcutaneous infusion, particularly at the 30 and 60 mpk doses. Therefore, in a subsequent PD study, 12 mpk was selected as the dose level.

**Table 1**  
In vitro SAR on human and mouse PrCP inhibition and mouse AngIII assays<sup>a</sup>

Compound No.		PrCP IC <sub>50</sub> (h, m) <sup>b</sup> , nM	Mouse AngIII IC <sub>50</sub> , nM
7a		10, –	>10000
7b		25, –	–
7c		93% at 5 μM, –	–
7d		141, –	–
7e		16, –	>10000
7f		18, –	290
7g		34, –	–
7h		22, 107	–
7i		129, –	–
7j		155, –	–
7k		42, –	–
7l		71, –	–
7m		30, –	2900
7n		64, –	–
7o		21, –	430
7p		93, –	–
7q		44, –	–
7r		24, –	8000

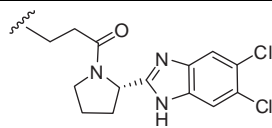
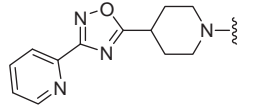
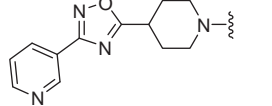
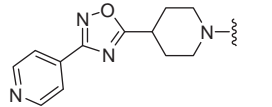
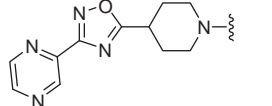
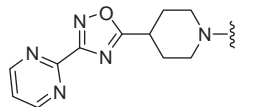
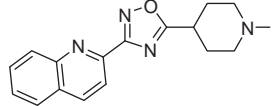
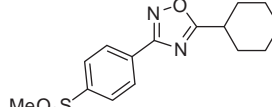
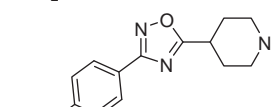
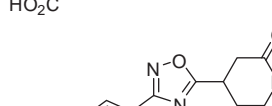
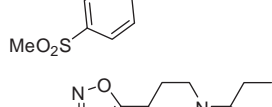
<sup>a</sup> Values are based on one or two experiments, each in triplicate.

<sup>b</sup> h = human, m = mouse.

In a seven-day pharmacodynamic (PD) study, food intake and body weight of the wild type and PrCP knockout eDIO mice<sup>13</sup> were measured daily during the continuous sc infusion of compound **9b** (12 mpk q.d.) and vehicle, respectively (Fig. 3). Despite the observation of a decrease in both food intake and body weight in the wild type group treated with compound **9b** (turquoise curve) with respect to the vehicle group (blue curve), the same magnitude of body weight and food intake effects were also manifested in the PrCP knockout group (lavender and red curves for vehicle and treated groups, respectively). This observation suggested that the body

weight and food intake effects of compound **9b** were not due to PrCP inhibition. At the end of the study, drug levels of all treated mice were obtained. It should be noted that only small differences were observed for the average drug levels of compound **9b** in the PrCP wild type and in knockout groups ( $0.21 \pm 0.10 \mu\text{M}$  in wild type vs  $0.29 \pm 0.14 \mu\text{M}$  in PrCP knockout mice,  $n = 8$ ). Comparing the drug level ( $0.21 \pm 0.10 \mu\text{M}$ ) with the vide supra target engagement study ( $\sim 50\%$  for drug exposure of  $0.09\text{--}0.16 \mu\text{M}$ ), it is reasonable to assume that  $\sim 50\%$  of plasma target engagement was achieved in this PD study. In light of this result and an earlier

**Table 2**  
In vitro SAR on human and mouse PrCP inhibition and mouse AngIII assays<sup>a</sup>

Compound No.		PrCP IC <sub>50</sub> (h, m) <sup>b</sup> , nM	Mouse AngIII IC <sub>50</sub> , nM
<b>8a</b>		12, 3.5	173
<b>8b</b>		18, –	155
<b>8c</b>		1.7, 0.53	29
<b>8d</b>		13, –	435
<b>8e</b>		19, –	745
<b>8f</b>		3.7, –	–
<b>8g</b>		2.3, 0.41	10
<b>8h</b>		17, –	241
<b>8i</b>		8.5, –	425
<b>8j</b>		15, 19	113

<sup>a</sup> Values are based on one or two experiments, each in triplicate.

<sup>b</sup> h = human, m = mouse.

observation that a PrCP inhibitor caused mechanism-based efficacy,<sup>12</sup> higher plasma target engagement is most likely required for PrCP-dependant weight loss. Thus, it would be more desirable to test compounds with good oral exposure and PrCP inhibitory activity via oral dosing to avoid compound precipitation and other potential side effects caused by continuous infusion.

As shown in Scheme 1, the synthesis of analog **9b** commenced with carboxylic acid **10**.<sup>14</sup> A Weinreb amide method provided methyl ketone intermediate **12**. This was followed by a Claisen condensation to yield diketone **14**. The subsequent condensation

with methylhydrazine afforded two pyrazole regioisomers. Compound **15**, the major regioisomer, was obtained by supercritical fluid chromatography using a chiral OJ column. Deprotection of the piperidine followed by a 1,4-addition to acrylate generated intermediate **17**, which then underwent ester cleavage and an ensuing amide formation using benzimidazole-substituted pyrrolidine **4**<sup>12</sup> to generate analog **9b**.

In conclusion, benzimidazole pyrrolidinyl amides containing a piperidinyl group have been shown to be a class of potent PrCP inhibitors in vitro. A representative compound (**9b**) displayed

**Table 3**  
In vitro SAR on human and mouse PrCP inhibition and mouse AngIII assays<sup>a</sup>

Compound No.		PrCP IC <sub>50</sub> (h, m) <sup>b</sup> , nM	Mouse AngIII IC <sub>50</sub> , nM
9a		4.7, –	–
9b		1.4, 0.8	6.7
9c		32, –	39
9d		27, –	485
9e		25, –	–
9f		7, –	–

<sup>a</sup> Values are based on one or two experiments, each in triplicate.

<sup>b</sup> h = human, m = mouse.

**Table 4**  
Mouse PK profiles of selected PrCP inhibitors<sup>a</sup>

Comps	F%	Cl (mL/min/kg)	Vd <sub>ss</sub> (L/kg)	T <sub>1/2</sub> (h)	AUCN <sub>po</sub> (μM h kg/mg)
8a	11	56	4.8	1.7	0.11
8c	8	38	5.7	4.9	0.07
8g	14	54	7.7	2.2	0.07
8i	3	115	3	1.3	0.007
8j	3	60	12	3.1	0.06
9b	4	65	9.4	4.1	0.02

<sup>a</sup> Formulations: 1 mg/mL ethanol/PEG/water (20:40:40). IV dose: 1 mg/kg (*n* = 2). PO dose: 2 mg/kg (*n* = 3). Blood concentration was determined by LC/MS/MS following protein precipitation with acetonitrile.

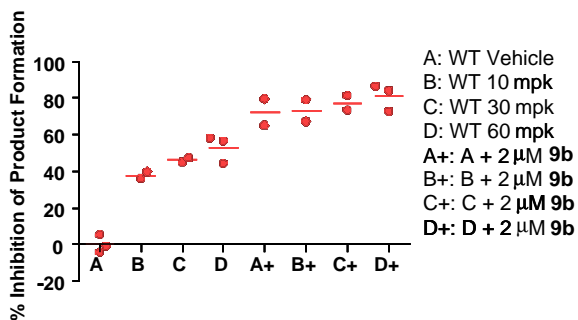


**Figure 2.** Target engagement of compound **9b** in wild type eDIO mouse (7th day, sc continuous pump infusion, normalized to vehicle).

excellent human PrCP inhibitory activity (IC<sub>50</sub> = 1 nM) and mouse whole serum PrCP inhibitory activity (IC<sub>50</sub> = 7 nM). It was found that this compound was a pgp substrate. Due to its suboptimal oral

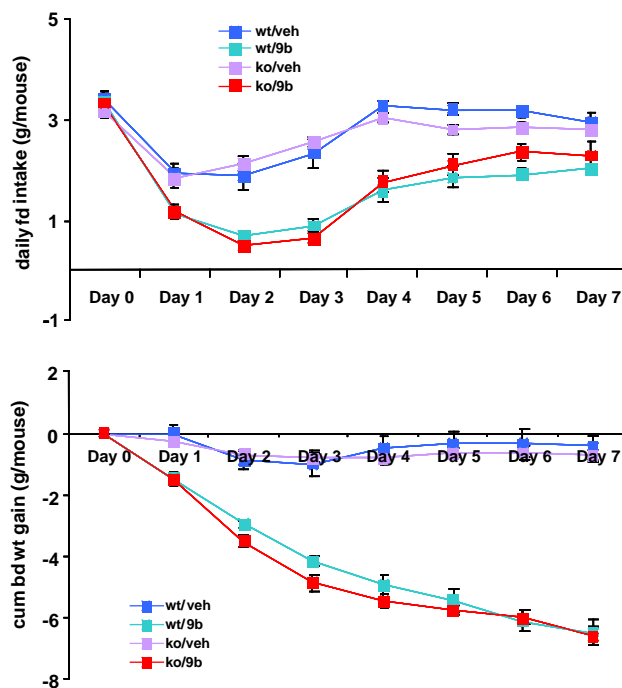
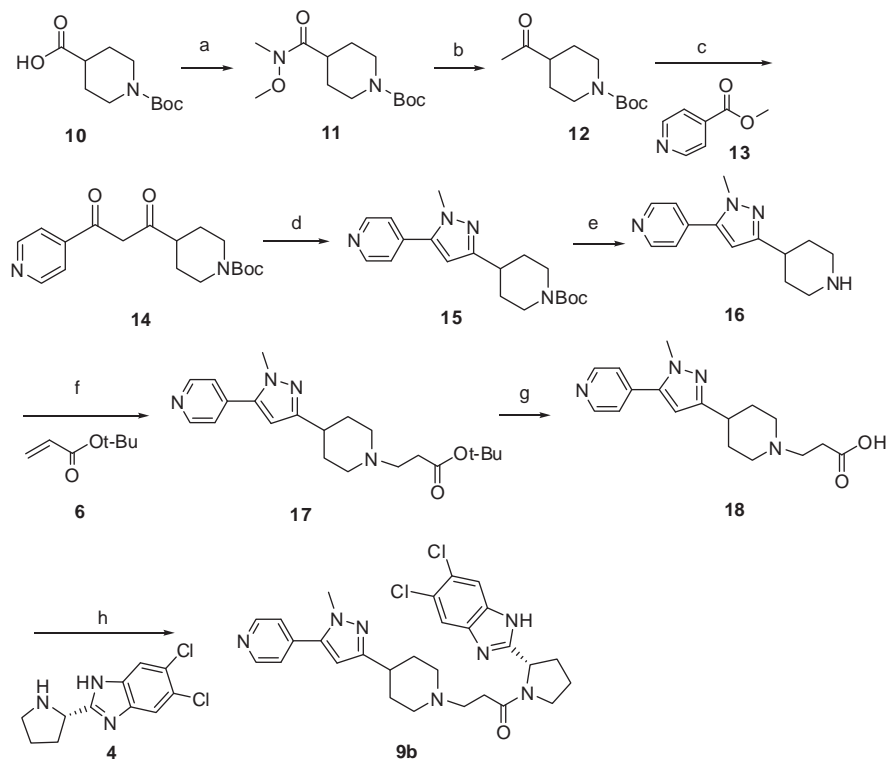


**Figure 3.** Compound **9b**-induced food intake and body weight loss of wild type eDIO mouse and PrCP knock/out eDIO mouse over seven days (*n* = 8 for all four groups; 12 mpk, sc continuous pump infusion; veh = vehicle, ko = PrCP knock out, wt = wild type; top: daily food intake (g/mouse), bottom: cumulative body weight gain (g/mouse)).



**Scheme 1.** Reagents and conditions: (a) MeNHOMe, EDC, Et<sub>3</sub>N, CH<sub>2</sub>Cl<sub>2</sub>, rt, 16 h, 77%; (b) MeMgBr, THF, –78 °C to 0 °C, 1 h, 96%; (c) **13**, NaH, THF, 0 °C to rt, 16 h, 75%; (d) MeNHNH<sub>2</sub>, EtOH, reflux, 2 h, chiral OJ column, 57%; (e) trifluoroacetic acid, CH<sub>2</sub>Cl<sub>2</sub>, rt, 1 h, 100%; (f) **6**, Et<sub>3</sub>N, CH<sub>3</sub>CN, 85 °C, 16 h, 92%; (g) trifluoroacetic acid, CH<sub>2</sub>Cl<sub>2</sub>, rt, 1 h, 100%; (h) **4**, EDC, HOBT, Et<sub>3</sub>N, CH<sub>2</sub>Cl<sub>2</sub>, rt, 5 h, 52%.

PK, **9b** was dosed at 12 mpk per day sc for seven days, and significantly reduced the body weight of the eDIO mice. However, analog **9b** also showed similar efficacy in PrCP knockout eDIO mice, suggesting that compound **9b**-induced weight loss in wild type eDIO mice was due to certain off-target effect. This result indicates that higher than 50% peripheral and/or certain level of central target engagement may be required to achieve efficacy.<sup>12</sup> The discovery of other structurally diverse and orally bioavailable PrCP inhibitors acting at peripheral and/or central tissues may better define the role of PrCP in regulating food intake and body weight. The results will be reported in due course.

## References and notes

- Yang, H. Y. T.; Erdos, E. G.; Chiang, T. S. *Nature* **1968**, *218*, 1224.
- Tan, F.; Morris, P. W.; Skidgel, R. A.; Erdos, E. G. *J. Biol. Chem.* **1993**, *268*, 16631.
- (a) Ody, C. E.; Marinkovic, D. V.; Hammon, K. J.; Stewart, T. A.; Erdos, E. G. *J. Biol. Chem.* **1978**, *253*, 5927; For a review: (b) Mallela, J.; Yang, J.; Shariat-Madar, Z. *Int. J. Biochem. Cell Biol.* **2008**, *41*, 477.
- (a) Kumamoto, K.; Stewart, T. A.; Johnson, A. R.; Erdős, E. G. *J. Clin. Invest.* **1981**, *67*, 210; (b) Skidgel, R. A.; Wickstrom, E.; Kumamoto, K.; Erdős, E. G. *Anal. Biochem.* **1981**, *118*, 113.
- Jackman, H. L.; Tan, F.; Schraufnagel, D.; Dragovic, T.; Dezso, B.; Becker, R. P.; Drdos, E. G. *Am. J. Respir. Cell Mol. Biol.* **1995**, *13*, 196.
- Watson, B.; Nowak, N. J.; Myracle, A. D.; Shows, T. B.; Warnock, D. G. *Genomics* **1997**, *44*, 365.
- Horvath, T.; Diano, S.; Gao, Q.; Warden, C. H. WO2005115446.
- Diament, A. L.; Warden, C. H. *Int. J. Obes. Relat. Metab. Disord.* **2004**, *28*, 199.
- McCarthy, J. J.; Meyer, J.; Moliterno, D. J.; Newby, L. K.; Rogers, W. J.; Topol, E. J. *Hum. Genet.* **2003**, *114*, 87.
- Chissoe, S. US20080108080.
- Palmiter, R. D. *J. Clin. Invest.* **2009**, *119*, 2130.
- Zhou, C.; Garcia-Calvo, M.; Pinto, S.; Lombardo, M.; Feng, Z.; Bender, K.; Pryor, K. D.; Bhatt, U. R.; Chabin, R. M.; Geissler, W. M.; Shen, Z.; Tong, X.; Zhang, X.; Wong, K. K.; Roy, S. S.; Chapman, K. T.; Yang, L.; Xiong, Y. *J. Med. Chem.* **2010**, *53*, 7251.
- Male C57BL/6NT wild-type and PrCP –/– mice (N6 C57BL/6NT background) were purchased from Taconic Farm, Inc.

- To the mixture of **10** (47.0 g, 205 mmol) and *N,O*-dimethylhydroxylamine hydrochloride (20.8 g, 213 mmol) in CH<sub>2</sub>Cl<sub>2</sub> (1 L) was added EDC (44.6 g, 232 mmol) in one portion followed by Et<sub>3</sub>N (32.4 mL, 232 mmol) dropwise at rt. The resulting solution was stirred at rt for 16 h. The solution was washed with brine (800 mL × 4) and a saturated NaHCO<sub>3</sub> solution (500 mL), and then dried over Na<sub>2</sub>SO<sub>4</sub>. After evaporating the solvent, the residue was purified on silica gel using 60% EtOAc/hexane to give **11** (43.2 g, 77%) as an oil. To the solution of **11** (43.2, 158 mmol) in THF (1.3 L) at –78 °C was added methylmagnesium bromide (106 mL, 3 M, 317 mmol) dropwise. The solution was warmed to 0 °C for 1 h before it was quenched with a saturated ammonium chloride solution. To this mixture was added EtOAc (1000 mL) and the organic phase was washed with brine (500 mL × 2), dried over Na<sub>2</sub>SO<sub>4</sub> to give **12** (34.8 g, 96%) as an oil. To the solution of **12** (7.99 g, 35.2 mmol) and **13** (5.78 g, 42.2 mmol) in THF (72 mL) was added NaH (1.69 g, 42.2 mmol, 60%) at 0 °C and the resulting mixture was stirred at rt for 16 h. The reaction mixture was cooled to –78 °C before it was quenched by methanol (7 mL) dropwise followed by the addition of saturated ammonium chloride solution (200 mL) at 0 °C. The resulting mixture was then extracted with EtOAc (200 mL × 3). The combined organic phase was washed with brine (500 mL), and dried over Na<sub>2</sub>SO<sub>4</sub>. After removing the volatile components, the residue was purified on silica gel eluting with 20–100% EtOAc/hexane to give **14** (8.75 g, 75%) as an oil. The solution of **14** (9.82 g, 29.5 mmol) and methyl hydrazine (1.90 mL, 35.5 mmol) in ethanol (250 mL) was heated at reflux for 2 h. After removing the volatile, the residue was purified on silica gel using EtOAc as the eluent to give a mixture of two regioisomers, which was further purified on chiral HPLC (OJ column, SFC method) using 25% MeOH/CO<sub>2</sub> to give pyrazole **15** (5.73 g, 57%) as a solid. To the solution of **15** (7.0 g, 20.4 mmol) in CH<sub>2</sub>Cl<sub>2</sub> (120 mL) was added trifluoroacetic acid (60 mL) and the resulting solution was stirred at rt for 1 h. After removing the volatile components, the residue was dissolved in CH<sub>2</sub>Cl<sub>2</sub> (300 mL), and washed with NaOH (500 mL, 2 N). The aqueous phase was extracted with CH<sub>2</sub>Cl<sub>2</sub> (300 mL × 3). The combined organic phase was dried over Na<sub>2</sub>SO<sub>4</sub> and concentrated to give **16** (5.15 g) as an oil. The solution of **16** (5.15 g, 21.3 mmol), Et<sub>3</sub>N (3.55 mL, 25.5 mmol), and **6** (9.25 mL, 63.8 mmol) in acetonitrile (200 mL) was heated at reflux for 16 h. The volatile components were evaporated and the residue was purified on silica gel using 2–10% MeOH/CH<sub>2</sub>Cl<sub>2</sub> to give **17** (7.24 g, 92% in two steps) as an oil. To the solution of **17** (4.38 g, 11.8 mmol) in CH<sub>2</sub>Cl<sub>2</sub> (10 mL) was added trifluoroacetic acid (32 mL) and the resulting solution was stirred at rt for 2 h. After removing the volatile components, the residue was dissolved in acetonitrile/water (2/1, 500 mL) and lyophilized to give **18** (7.37 g, 95%) as a TFA salt.

To the solution of **18** (5.03, 7.66 mmol), **4** (3.78 g, 11.5 mmol), HOBT (1.17 g, 7.66 mmol), and Et<sub>3</sub>N (8.54 mL, 61.3 mmol) in CH<sub>2</sub>Cl<sub>2</sub> (100 mL) was added EDC (2.94 g, 15.3 mmol), and the resulting solution was stirred at rt for 4 h. The reaction solution was then diluted with CH<sub>2</sub>Cl<sub>2</sub> (600 mL), washed with saturated NaHCO<sub>3</sub> (500 mL × 3), and dried over Na<sub>2</sub>SO<sub>4</sub>. After evaporating the volatile, the residue was purified on silica gel using 5–20% MeOH/CH<sub>2</sub>Cl<sub>2</sub> (0.25% Et<sub>3</sub>N) to give **9b** (2.22 g, 52%) as a white foam. <sup>1</sup>H NMR (chloroform-*d*,

500 MHz): δ 8.70 (d, *J* = 6.2 Hz, 2H), 7.82 (s, 1H), 7.54 (s, 1H), 7.36 (d, *J* = 6.0 Hz, 2H), 6.24 (s, 1H), 5.44–5.42 (m, 1H), 3.93 (s, 3H), 3.74–3.64 (m, 1H), 3.61–3.56 (m, 1H), 3.17–3.09 (m, 2H), 3.01–2.94 (m, 1H), 2.88–2.75 (m, 4H), 2.64–2.61 (m, 1H), 2.42–2.23 (m, 4H), 2.17–2.12 (m, 1H), 2.12–2.05 (m, 2H), 1.85–1.85 (m, 2H). Exact mass calcd for C<sub>28</sub>H<sub>31</sub>Cl<sub>2</sub>N<sub>7</sub>O: 551.2 (100%); 553.2 (64%); found [M+H]<sup>+</sup>: 552.1 (100%); 554.0 (66%).